Pseudorapidity dependence of anisotropic flows in relativistic heavy-ion collisions

Lie-Wen Chen,[1,2] Vincenzo Greco,[2] Che Ming Ko,[2] and Peter F. Kolb[3]

[1]*Department of Physics, Shanghai Jiao Tong University, Shanghai 200030, China*
[2]*Cyclotron Institute and Physics Department, Texas A&M University, College Station, Texas 77843-3366*
[3]*Physik Department, Technische Universität München, D-85747 Garching, Germany*

(Dated: July 22, 2018)

The pseudorapidity dependence of anisotropic flows v_1, v_2, v_3, and v_4 of charged hadrons in heavy-ion collisions at the Relativistic Heavy Ion Collider is studied in a multi-phase transport model. We find that while the string melting scenario, in which hadrons that are expected to be formed from initial strings are converted to their valence quarks and antiquarks, can explain the measured p_T-dependence of v_2 and v_4 of charged hadrons at midrapidity with a parton scattering cross section of about 10 mb, the scenario without string melting reproduces better the recent data on v_1 and v_2 of charged hadrons at large pseudorapidity in Au + Au collisions at $\sqrt{s} = 200$ AGeV. Our results thus suggest that a partonic matter is formed during early stage of relativistic heavy ion collisions only around midrapidity and that strings remain dominant at large rapidities. The p_T-dependence of v_1, v_2, v_3 and v_4 for charged hadrons at forward pseudorapidity is also predicted, and we find that while v_1 and v_2 are appreciable at large pseudorapidity the higher-order anisotropic flows v_3 and v_4 are essentially zero.

PACS numbers: 25.75.Ld, 24.10.Lx

I. INTRODUCTION

Anisotropic flows in heavy ion collisions [1, 2, 3, 4], which have been studied extensively at the Relativistic Heavy Ion Collider (RHIC), are sensitive to the properties of produced matter. This sensitivity not only exists in the larger elliptic flow [5, 6, 7, 8, 9, 10, 11, 12] but also in the smaller higher-order anisotropic flows [13, 14, 15, 16, 17, 18, 19]. Furthermore, scaling relations among hadron anisotropic flows are observed in the experimental data [17], and they are shown in theoretical models to relate to similar scaling relations among parton elliptic flows [18, 19]. These studies have, however, mainly focused on hadrons at mid-rapidity where odd-order anisotropic flows vanish in collisions of equal mass nuclei. Recently, anisotropic flows at finite pseudorapidities have also been measured in Au + Au collisions at RHIC. The experimental results show that both v_1 and v_2 depend strongly on the rapidity [17, 20, 21, 22, 23, 24], and this has so far not been reproduced by theoretical models [25, 26, 27]. These new experimental data thus offer the opportunity to test the validity of theoretical models and to study the dynamics and properties of produced matter at large rapidity in heavy ion collisions at RHIC.

In the present work, we shall use a multi-phase transport (AMPT) model, that includes both initial partonic and final hadronic interactions [28, 29], to study the pseudorapidity dependence of anisotropic flows v_1, v_2, v_3, and v_4 of charged hadrons in heavy-ion collisions at RHIC. Both the default version and the version with string melting, i.e., allowing hadrons that are expected to be formed from initial strings to convert to their valence quarks and antiquarks [10, 30, 31], will be used. The latter was able to explain the measured p_T dependence of v_2 and v_4 of mid-rapidity charged hadrons with a parton scattering cross section of about 10 mb. We find in the present study that the same parton cross section fails to reproduce recent data on v_1 and v_2 at large pseudorapidity in Au + Au collisions at $\sqrt{s} = 200$ AGeV. These data are explained instead by the default scenario without string melting. Our results thus suggest that a pure partonic matter is formed only near midrapidity during the early stage of these collisions, and the matter at large pseudorapidity remains dominated by strings. We also give predictions on the p_T-dependence of v_1, v_2, v_3 and v_4 at forward pseudorapidity.

II. THE AMPT MODEL

The AMPT model [28, 29, 32, 33] is a hybrid model that uses minijet partons from hard processes and strings from soft processes in the Heavy Ion Jet Interaction Generator (HIJING) model [34] as the initial conditions for modeling heavy ion collisions at ultra-relativistic energies. Time evolution of resulting minijet partons is then described by Zhang's parton cascade (ZPC)[35] model. At present, this model includes only parton-parton elastic scatterings with an in-medium cross section given by:

$$\frac{d\sigma_p}{dt} = \frac{9\pi\alpha_s^2}{2}\left(1+\frac{\mu^2}{s}\right)\frac{1}{(t-\mu^2)^2}, \qquad (1)$$

where the strong coupling constant α_s is taken to be 0.47, and s and t are usual Mandelstam variables. The effective screening mass μ depends on the temperature and density of the partonic matter but is taken as a parameter in ZPC for fixing the magnitude and angular distribution of parton scattering cross section. After minijet partons stop interacting, they are combined with their parent strings, as in the HIJING model with jet quenching, to fragment into hadrons using the Lund string fragmentation model

as implemented in the PYTHIA program [36]. The final-state hadronic scatterings are then modeled by a relativistic transport (ART) model [37]. The default AMPT model [28] has been quite successful in describing measured rapidity distributions of charge particles, particle to antiparticle ratios, and spectra of low transverse momentum pions and kaons [29] in heavy ion collisions at the Super Proton Synchrotron (SPS) and RHIC. It has also been useful in understanding the production of J/ψ [32] and multistrange baryons [33] in these collisions.

Since the initial energy density in Au + Au collisions at RHIC is much larger than the critical energy density at which the hadronic matter to quark-gluon plasma transition would occur [32, 38], the AMPT model has been extended to convert the initial excited strings into partons [10]. In this string melting scenario, hadrons (mostly pions), that would have been produced from string fragmentation, are converted instead to valence quarks and/or antiquarks with current quark masses. Interactions among these partons are again described by the ZPC parton cascade model. Since there are no inelastic scatterings, only quarks and antiquarks from the melted strings are present in the partonic matter. The transition from the partonic matter to the hadronic matter is then achieved using a simple coalescence model, which combines two nearest quark and antiquark into mesons and three nearest quarks or antiquarks into baryons or anti-baryons that are close to the invariant mass of these partons. The present coalescence model is thus somewhat different from the ones recently used extensively [39, 40, 41, 42] for studying hadron production at intermediate transverse momenta. Using parton scattering cross sections of 6-10 mb, the AMPT model with string melting is able to reproduce both the centrality and transverse momentum (below 2 GeV/c) dependence of the elliptic flow [10] and pion interferometry [30] measured in Au+Au collisions at $\sqrt{s} = 130$ AGeV at RHIC [43, 44]. It has also been used for studying the kaon interferometry in these collisions [45]. We note that the above cross sections are significantly smaller than that needed to reproduce the parton elliptic flow from the hydrodynamic model [46]. The resulting hadron elliptic flows in the AMPT model with string melting are, however, amplified by modeling hadronization via quark coalescence [42], leading to a satisfactory reproduction of experimental data.

III. TRANSVERSE MOMENTUM SPECTRA

We first show in Fig.1 the pion and kaon transverse momentum spectra at rapidity $y = 0$ and 3 in central Au+Au collisions at $\sqrt{s} = 200$ AGeV. Compared to experimental data from the BRAHMS collaboration [47], shown by squares for pions and triangles for kaons, the default AMPT model shown by solid curves reproduces them well, but the AMPT model with string melting, on the other hand, gives a smaller inverse slope parameter for both parton cross sections of $\sigma_p = 3$ mb (dotted curves) and 10 mb (dashed curves). The reason that hadron transverse momentum spectra are softened in the string melting scenario is due to a softer initial parton spectra obtained from converting hadrons to quarks and antiquarks, and the small current quark masses that make their transverse momentum spectra less affected by radial collective flow than hadrons in the default AMPT model. Since hadron anisotropic flows are given by ratios of hadron momentum distributions in the transverse plane, the AMPT model with string melting is expected to give a reliable prediction [10].

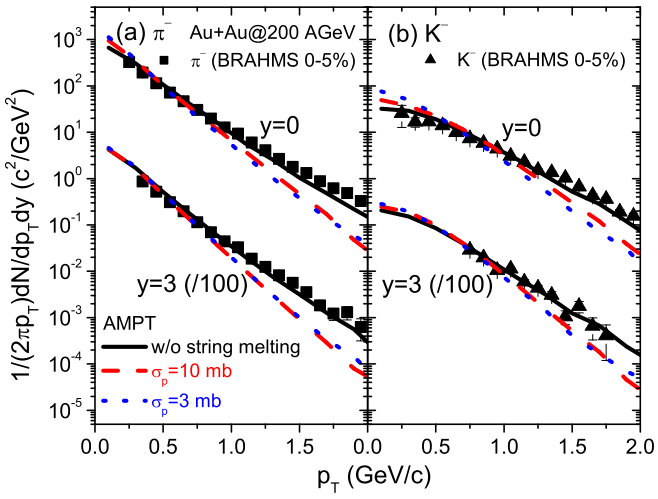

FIG. 1: (Color online) Pion and kaon transverse momentum spectra at rapidity $y = 0$ and 3 in central Au+Au collisions at $\sqrt{s} = 200$ AGeV. Solid curves are from default AMPT model, while dotted and dashed curves are from AMPT model with string melting using parton cross section $\sigma_p = 3$ mb and 10 mb, respectively. Experimental data from the BRAHMS collaboration [47] are squares for pions and triangles for kaons.

IV. ANISOTROPIC FLOWS

The anisotropic flows v_n of particles are the Fourier coefficients in the decomposition of their transverse momentum spectra in the azimuthal angle ϕ with respect to the reaction plane [48], i.e.,

$$E\frac{d^3N}{dp^3} = \frac{1}{2\pi}\frac{dN}{p_T dp_T dy}[1 + \sum_{n=1}^{\infty} 2v_n(p_T, y)\cos(n\phi)] \quad (2)$$

Because of the symmetry $\phi \leftrightarrow -\phi$ in the collision geometry, no sine terms appear in the above expansion. For particles at midrapidity in collisions with equal mass nuclei, anisotropic flows of odd orders vanish as a result of the additional symmetry $\phi \leftrightarrow \phi + \pi$. The anisotropic flows generally depend on particle transverse momentum and rapidity, and for a given rapidity the anisotropic

flows at transverse momentum p_T can be evaluated according to

$$v_n(p_T) = \langle \cos(n\phi) \rangle \,, \tag{3}$$

where $\langle \cdots \rangle$ denotes average over the azimuthal distribution of particles with transverse momentum p_T. The anisotropic flows v_n can further be expressed in terms of the single-particle averages:

$$v_1(p_T) = \left\langle \frac{p_x}{p_T} \right\rangle \tag{4}$$

$$v_2(p_T) = \left\langle \frac{p_x^2 - p_y^2}{p_T^2} \right\rangle \tag{5}$$

$$v_3(p_T) = \left\langle \frac{p_x^3 - 3p_x p_y^2}{p_T^3} \right\rangle \tag{6}$$

$$v_4(p_T) = \left\langle \frac{p_x^4 - 6p_x^2 p_y^2 + p_y^4}{p_T^4} \right\rangle \tag{7}$$

where p_x and p_y are, respectively, the projections of particle momentum in and perpendicular to the reaction plane.

V. PSEUDORAPIDITY DEPENDENCE OF ANISOTROPIC FLOWS

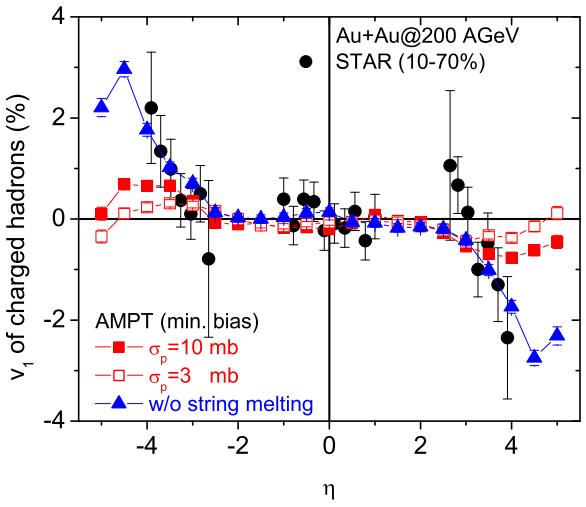

FIG. 2: (Color online) Pseudorapidity dependence of v_1 from minimum bias events of Au + Au collisions at $\sqrt{s} = 200$ AGeV in the string melting scenario with parton scattering cross sections $\sigma_p = 3$ (open squares) and 10 (solid squares) mb as well as the scenario without string melting (triangles). Data are from the STAR collaboration (circles) [17].

In Fig. 2, we show the pseudorapidity dependence of v_1 for charged hadrons from minimum bias events of Au + Au collisions at $\sqrt{s} = 200$ AGeV by using the string melting scenario with parton scattering cross sections $\sigma_p = 3$ (open squares) and 10 mb (solid squares) and the scenario without string melting (default AMPT model, triangles). Also included in Fig. 2 are recent data from the STAR collaboration (circles) [17]. Both scenarios can reproduce approximately the data around the mid-pseudorapidity region, i.e., v_1 is flat (essentially zero) around mid-η. For v_1 at large $|\eta|$, the string melting scenario with both parton scattering cross sections $\sigma_p = 3$ mb and 10 mb underestimates significantly the data. On the other hand, the scenario without string melting seems to give a good description of v_1 at large $|\eta|$. Our results thus indicate that the matter produced at large $|\eta|$ ($|\eta| \geq 3$) at RHIC initially consists of mostly strings instead of partons. This is a reasonable picture as particles at large rapidity are produced later in time when the volume of the system is large and the energy density is small.

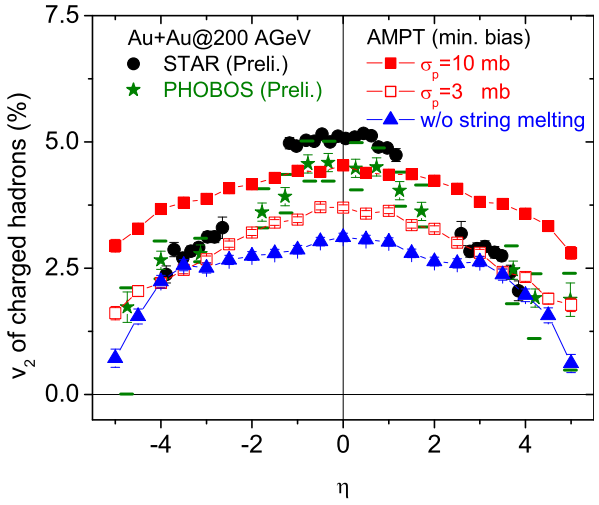

FIG. 3: (Color online) Pseudorapidity dependence of v_2 from minimum bias events of Au + Au collisions at $\sqrt{s} = 200$ AGeV in the string melting scenario with parton scattering cross sections $\sigma_p = 3$ (open squares) and 10 (solid squares) mb as well as the scenario without string melting (triangles). Data are from the PHOBOS (stars) [21] and STAR collaborations (circles) [23].

The predicted pseudorapidity dependence of charged hadron v_2 from the same reaction is shown in Fig. 3, together with preliminary data from the PHOBOS collaboration (stars) [21] and the STAR collaboration (circles) [23]. One sees that the string melting scenario with $\sigma_p = 10$ mb (solid squared) describes very well the data on v_2 around mid-η ($|\eta| \leq 1.5$) while it overestimates the data at large pseudorapidity. Surprisingly, the calculated results with $\sigma_p = 10$ mb are similar to the prediction from the hydrodynamic model that includes the "thermalization coefficient" correction [26]. The overestimation of v_2 for charged hadrons at large pseudorapidity ($|\eta| \gtrsim 1.5$) obtained with $\sigma_p = 10$ mb may be due to the constant parton scattering cross section used in the calculations. As shown in Eq.(1), the parton scattering cross section depends on the gluon screening mass and is thus temper-

ature and density dependent. Since the dynamics of partonic matter at different rapidities may not be the same in heavy ion collisions at RHIC, different parton cross sections may have to be used. Comparison between theoretical results and the experimental data on elliptic flow indicates that a larger $\sigma_p = 10$ mb is needed at midrapidity but a smaller $\sigma_p = 3$ mb (open squares) gives a better description at large pseudorapidity. Also shown in Fig. 3 are results obtained from the scenario without string melting (triangles), and they are seen to also describe the data at large pseudorapidity ($|\eta| \geqslant 3$). Therefore, the scenario without string melting can describe simultaneously the data for v_1 and v_2 at large pseudorapidity ($|\eta| \geqslant 3$). These interesting features imply that initially the matter produced at large pseudorapidity ($|\eta| \geqslant 3$) is dominated by strings while that produced around midrapidity ($|\eta| \leq 3$) mainly consists of partons.

VI. p_T-DEPENDENCE OF ANISOTROPIC FLOWS AT FORWARD RAPIDITY

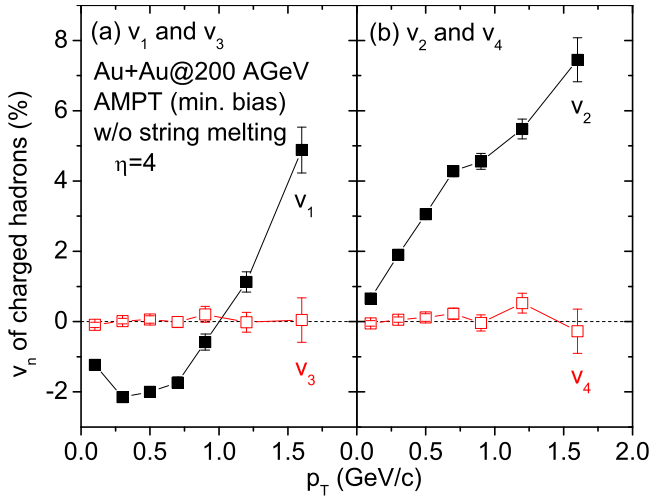

FIG. 4: (Color online) Transverse momentum dependence of v_1 and v_3 (a) as well as v_2 and v_4 (b) for charged hadrons at forward pseudorapidity ($\eta = 4$) from minimum bias events of Au + Au collisions at $\sqrt{s} = 200$ AGeV from the default AMPT model without string melting.

More detailed information about anisotropic flows can be obtained from the differential anisotropic flows, i.e., their p_T dependence. Using the scenario without string melting, we show in Fig. 4 the p_T-dependence of v_1, v_2, v_3, and v_4 for charged hadrons at forward pseudorapidity ($\eta = 4$) from minimum bias events of Au + Au collisions at $\sqrt{s} = 200$ AGeV. It is seen that the directed flow $v_1(p_T)$ shown in Fig. 4 (a) is non-zero and changes from negative to positive values at a balance transverse momentum of about 1.0 GeV/c. This feature implies that charged hadrons with lower and higher transverse momentum move preferentially towards the negative and positive transverse flow direction, respectively, consistent with that seen in the hydrodynamic model [26]. The p_T-integrated directed flow v_1 can be non-zero at large η as already shown in Fig. 2. The differential anisotropic flow, however, allows one to learn in more detail the dynamics of heavy ion collisions. The $v_3(p_T)$ shown in Fig. 4 (a) is essentially zero. Fig. 4 (b) shows the differential elliptic flow $v_2(p_T)$ and $v_4(p_T)$ at $\eta = 4$. A strong elliptic flow $v_2(p_T)$ is observed while $v_4(p_T)$ is again almost zero (less than 0.5%), which is consistent with preliminary data from the STAR collaboration [23]. Comparison of our predictions with future data can test the conclusion that the matter produced at large pseudorapidity ($|\eta| \geqslant 3$) in the early stage of collisions is dominated by strings. In this case, it would be interesting to see experimentally if the constituent quark number scaling of meson and baryon elliptic flows seen at midrapidity is indeed not valid at large pseudorapidity.

VII. SUMMARY

In summary, using the AMPT model, we have studied the pseudorapidity dependence of anisotropic flows v_1, v_2, v_3, and v_4 of charged hadrons in heavy-ion collisions at RHIC. Within the string melting scenario, we find that a parton scattering cross section of about 10 mb, that is used in explaining the measured p_T-dependence of v_2 and v_4 for charged hadrons at midrapidity, fails to reproduce recent data on their v_1 and v_2 at large pseudorapidity from Au + Au collisions at $\sqrt{s} = 200$ AGeV. Allowing a smaller parton cross section at large pseudorapidity, the measured pseudorapidity dependence of v_2 could be quantitatively accounted for but the v_1 at large pseudorapidity ($|\eta| \geqslant 3$) is still underestimated. We further find that v_1 and v_2 at large pseudorapidity can be described simultaneously by the scenario without string melting. Our results thus suggest that the matter produced at large pseudorapidity ($|\eta| \geqslant 3$) during the early stage of Au + Au collisions at $\sqrt{s} = 200$ AGeV is dominated by strings while that produced around mid-pseudorapidity ($|\eta| \leq 3$) consists mainly of partons. The predicted p_T-dependence of v_1, v_2, v_3 and v_4 at forward pseudorapidity shows that there exist strong directed flow v_1 and elliptic flow v_2 while v_3 and v_4 are essentially zero. Experimental verification of these predictions at RHIC will be useful in testing the AMPT model and in understanding how the collision dynamics changes with rapidity.

Acknowledgments

This paper was based on work supported in part by the US National Science Foundation under Grant No. PHY-0098805 and the Welch Foundation under Grant No. A-1358 (LWC,VG,CMK), the National Science Foundation of China under Grant No. 10105008 (LWC), the National Institute of Nuclear Physics (INFN) in Italy (VG), and

the BMBF and the DFG (PK).

[1] J.Y. Ollitrault, Phys. Rev. D 46 (1992) 229.
[2] H. Sorge, Phys. Lett. B 402 (1997) 251; Phys. Rev. Lett. 78 (1997) 2309;
H. Sorge, Phys. Rev. Lett. 82 (1999) 2048.
[3] P. Danielewicz, R.A. Lacey, P.B. Gossiaux, C. Pinkenburg, P. Chung, J. M. Alexander, and R.L. McGrath, Phys. Rev. Lett. 81 (1998) 2438.
[4] Y. Zheng, C.M. Ko, B.A. Li, and B. Zhang, Phys. Rev. Lett. 83 (1999) 2534.
[5] D. Teaney, J. Laureant, and E.V. Shuryak, Phys. Rev. Lett. 86 (2001) 4783.
[6] P.F. Kolb, P. Huovinen, U. Heinz, and H. Heiselberg, Phys. Lett. B 500 (2001) 232.
[7] P. Huovinen, P.F. Kolb, U. Heinz, P.V. Ruuskanen, and S. Voloshin, Phys. Lett. B 503 (2001) 58.
[8] B. Zhang, M. Gyulassy, and C.M. Ko, Phys. Lett. B 455 (1999) 45.
[9] D. Molnar and M. Gyulassy, Nucl. Phys. A 698 (2002) 379.
[10] Z.W. Lin and C.M. Ko, Phys. Rev. C 65 (2002) 034904.
[11] M. Gyulassy, I. Vitev and X.N. Wang, Phys. Rev. Lett. 86 (2001) 2537.
[12] S.A. Voloshin, Nucl. Phys. A 715 (2003) 379c.
[13] P.F. Kolb, J. Sollfrank, and U. Heinz, Phys. Lett. B 459 (1999) 667.
[14] D. Teaney and E.V. Shuryak, Phys. Rev. Lett. 83 (1999) 4951.
[15] P.F. Kolb, J. Sollfrank, and U. Heinz, Phys. Rev. C 62 (2000) 054909.
[16] P.F. Kolb, Phys. Rev. C 68 (2003) 031902(R).
[17] J. Adams et al. [STAR Collaboration], Phys. Rev. Lett. 92 (2004) 062301.
[18] L.W. Chen, C.M. Ko, and Z.W. Lin, Phys. Rev. C 69 (2004) 031901(R).
[19] P. Kolb, L.W. Chen, V. Greco, and C.M. Ko, Phys. Rev. C 69 (2004) 051901(R).
[20] B.B. Back et al., Phys. Rev. Lett. 89 (2002) 222301.
[21] S. Manly for the PHOBOS Collaboration, Nucl. Phys. A 715 (2003) 611c.
[22] M.B. Tonjes for the PHOBOS Collaboration, nucl-ex/0403025.
[23] M. D. Oldenberg for the STAR Collaboration, 2004, nucl-ex/0403007.
[24] B.B. Back et al., nucl-ex/0407012.
[25] T. Hirano, Phys. Rev. C 65 (2001) 011901(R).
[26] U. Heinz and P.F. Kolb, J. Phys. G 30 (2004) S1229.
[27] M. Csanad, T. Csorgo, B. Lorstad, and A. Ster, J. Phys. G 30 (2004) S1079;
M. Csanad, T. Csorgo, and B. Lorstad, nucl-th/0310040.
[28] B. Zhang, C.M. Ko, B.A. Li, and Z.W. Lin, Phys. Rev. C 61 (2000) 067901.
[29] Z.W. Lin, S. Pal, C.M. Ko, B.A. Li, and B. Zhang, Phys. Rev. C 64 (2001) 011902;
Z.W. Lin, S. Pal, C.M. Ko, B.A. Li, and B. Zhang, Nucl. Phys. A 698 (2002) 375.
[30] Z.W. Lin, C.M. Ko, and S. Pal, Phys. Rev. Lett. 89 (2002) 152301.
[31] C.M. Ko, Z.W. Lin, and S. Pal, Heavy Ion Phys. 17 (2003) 219.
[32] B. Zhang, C.M. Ko, B.A. Li, Z.W. Lin, and B.H. Sa, Phys. Rev. C 62 (2002) 054905;
B. Zhang, C.M. Ko, B.A. Li, Z.W. Lin, and S. Pal, Phys. Rev. C 65 (2002) 054909.
[33] S. Pal. C.M. Ko, and Z.W. Lin, Nucl. Phys. A 730 (2004) 143.
[34] X.N. Wang and M. Gyulassy, Phys. Rev. D 44 (1991) 3501.
[35] B. Zhang, Comput. Phys. Commun. 109 (1998) 193.
[36] T. Sjostrand, Comput. Phys. Commun. 82 (1994) 74.
[37] B.A. Li and C.M. Ko, Phys. Rev. C 52 (1995) 2037;
B.A. Li, A.T. Sustich, B. Zhang, and C.M. Ko, Int. Jour. Phys. E 10 (2001) 267.
[38] D. Kharzeev and M. Nardi, Phys. Lett. B 507 (2001) 121.
[39] V. Greco, C.M. Ko, and P. Lévai, Phys. Rev. Lett. 90 (2003) 202302;
V. Greco, C.M. Ko, and P. Lévai, Phys. Rev. C 68 (2003) 034904.
[40] R.C. Hwa and C.B. Yang, Phys. Rev. C 67 (2003) 034902;
R.C. Hwa and C.B. Yang, Phys. Rev. C 67 (2003) 064902.
[41] R.J. Fries, B. Müller, C. Nonaka, and S.A. Bass, Phys. Rev. Lett. 90 (2003) 202303;
R.J. Fries, B. Müller, C. Nonaka, and S.A. Bass, Phys. Rev. C 68 (2003) 044902.
[42] D. Molnar and S.A. Voloshin, Phys. Rev. Lett. 91 (2003) 092301.
[43] K.H. Ackermann et al. [STAR Collaboration], Phys. Rev. Lett. 86 (2001) 402.
[44] C. Adler et al. [STAR Collaboration], Phys. Rev. Lett. 87 (2001) 082301.
[45] Z.W. Lin and C.M. Ko, J. Phys. G 30 (2004) S263.
[46] D. Molnar and P. Huovinen, nucl-th/0404065.
[47] I.G. Bearden et al. [BRAHMS Collaboration], nucl-ex/0403050.
[48] A.M. Poskanzer and S.A. Voloshin, Phys. Rev. C 58 (1998) 1671.